Title

Gut Microbiota from Twins Discordant for Obesity Modulate Metabolism in Mice

Journal

Science, 341(6150)

ISSN

0036-8075

Authors

Ridaura, Vanessa K

Faith, Jeremiah J

Rey, Federico E

et al.

Publication Date

2013-09-06

DOI

10.1126/science.1241214

Peer reviewed

Published in final edited form as:
Science. 2013 September 6; 341(6150): . doi:10.1126/science.1241214.

Cultured gut microbiota from twins discordant for obesity modulate adiposity and metabolic phenotypes in mice

Vanessa K. Ridaura[1], **Jeremiah J. Faith**[1], **Federico E. Rey**[1], **Jiye Cheng**[1], **Alexis E. Duncan**[2,3], **Andrew L. Kau**[1], **Nicholas W. Griffin**[1], **Vincent Lombard**[4], **Bernard Henrissat**[4,5], **James R. Bain**[6,7,8], **Michael J. Muehlbauer**[6], **Olga Ilkayeva**[6], **Clay F. Semenkovich**[9], **Katsuhiko Funai**[9], **David K. Hayashi**[10], **Barbara J. Lyle**[11], **Margaret C. Martini**[11], **Luke K. Ursell**[12], **Jose C. Clemente**[12], **William Van Treuren**[12], **William A. Walters**[13], **Rob Knight**[12,14,15], **Christopher B. Newgard**[6,7,8], **Andrew C. Heath**[2], and **Jeffrey I. Gordon**[1,*]

[1]Center for Genome Sciences and Systems Biology, Washington University School of Medicine, St. Louis, MO 63108 USA

[2]Department of Psychiatry, Washington University School of Medicine, St. Louis, MO 63110 USA

[3]George Warren Brown School of Social Work, Washington University, St. Louis, MO 63130 USA

[4]Aix Marseille Université, CNRS UMR 7257, 13288 Marseille, France

[5]Department of Cellular and Molecular Medicine, Faculty of Health and Medical Sciences, University of Copenhagen, DK-2200, Copenhagen, Denmark

[6]Sarah W. Stedman Nutrition and Metabolism Center, Duke University Medical Center, Durham, NC 27710 USA

[7]Department of Medicine, Duke University Medical Center, Durham, NC 27710 USA

[8]Department of Pharmacology and Cancer Biology, Duke University Medical Center, Durham, NC 27710 USA

[9]Department of Medicine, Washington University School of Medicine, St. Louis, MO 63110 USA

[10]Mondelez International, Glenview, IL 60025 USA

[11]Kraft Foods Group, Glenview, IL 60025 USA

[12]Department of Chemistry & Biochemistry, Univ. of Colorado, Boulder, CO 80309 USA

[13]Department of Molecular, Cellular and Developmental Biology, Univ. of Colorado, Boulder, CO 80309 USA

[14]Biofrontiers Institute, Univ. of Colorado, Boulder, CO 80309 USA

[*]To whom correspondence should be sent. jgordon@wustl.edu.

Author contributions:
V.K.R. and J.I.G designed the mouse experiments, A.C.H., A.E.D. and J.I.G. designed and implemented the clinical data collection, N.W.G., D.K.H., B.J.L., and M.C.M designed the NHANES-based mouse diets, V.K.R., J.J.F., J.C., M.J.M, J.R.B., K.F. and O.I. generated the data, V.K.R., J.J.F., F.R., J.C., J.C.C., W.V.T, L.K.U., W.A.W., A.K., R.K., A.E.D., A.C.H., B.H., V.L., M.J.M., J.R.B., C.B.N., and J.I.G. analyzed the data, and V.K.R. and J.I.G. wrote the paper.

Supplementary Materials
www.sciencemag.org
Materials and Methods
Supplementary Results
Supplementary figs. S1 to S17
Supplementary tables S1 to S17
Supplementary references (50–76)

[15]Howard Hughes Medical Institute, Univ. of Colorado, Boulder, CO 80309 USA

Abstract

The role of specific gut microbes in shaping body composition remains unclear. We transplanted fecal microbiota from adult female twin pairs discordant for obesity into germ-free mice fed low-fat mouse chow, as well as diets representing different levels of saturated fat and fruit and vegetable consumption typical of the USA. Increased total body and fat mass, as well as obesity-associated metabolic phenotypes were transmissible with uncultured fecal communities, and with their corresponding fecal bacterial culture collections. Co-housing mice harboring an obese twin's microbiota (Ob) with mice containing the lean co-twin's microbiota (Ln) prevented the development of increased body mass and obesity-associated metabolic phenotypes in Ob cagemates. Rescue correlated with invasion of specific members of Bacteroidetes from the Ln microbiota into Ob microbiota, and was diet-dependent. These findings reveal transmissible, rapid and modifiable effects of diet-by-microbiota interactions.

Microbial community configurations vary substantially between unrelated individuals (1–9), creating a challenge in designing surveys of sufficient power to determine whether observed differences between disease-associated and healthy communities differ significantly from normal interpersonal variation. This challenge is especially great if, for a given disease state, there are many associated states of the microbial species (microbiota) or microbial gene repertoire (microbiome), each shared by relatively few individuals. Microbiota configurations are influenced by early environmental exposures and are generally more similar among family members (2, 7, 10, 11).

There have been conflicting reports about the relationship between interpersonal differences in the structure of the gut microbiota (e.g., the representation of Bacteroidetes and Firmicutes) and host body mass index (BMI). Taxonomic profiles for obese and lean individuals may have distinct patterns between human populations, but technical issues related to how gut samples are processed and community members are identified by 16S rRNA gene sequencing may also play a role in observed differences. The relative contributions of the microbiome and dietary components to obesity and obesity-related metabolic phenotypes are unclear and likely multifaceted (2, 12–17). Transplants of fecal microbiota from healthy donors to recipients with metabolic syndrome have provided evidence that the microbiota can ameliorate insulin-resistance, although the underlying mechanisms remain unclear (18).

Monozygotic (MZ) or dizygotic (DZ) twins discordant for obesity (19, 20) provide an attractive model for studying the interrelationships between obesity, its associated dietary and lifestyle risk factors, and the gut microbiome. In the case of same-sex twins discordant for a disease phenotype, the healthy co-twin provides a valuable reference control to contrast with the co-twin's disease-associated gut community. However, this comparison is fundamentally descriptive and cannot establish causality. Transplanting a fecal sample obtained from each twin in a discordant pair into separate groups of recipient germ-free mice provides an opportunity to: (i) identify structural and functional differences between their gut communities; (ii) generate and test hypotheses about the impact of these differences on host biology, including body composition and metabolism; and (iii) determine the effects of diet-by-microbiota interactions through manipulation of the diets fed to these 'humanized' animals and/or the representation of microbial taxa in their gut communities.

Reproducibility of microbiota transplants from discordant twins

We surveyed data collected from 1,539 21–32 year-old female twin pairs enrolled in the Missouri Adolescent Female Twin Study [MOAFTS; (21, 22)]; for further details see ref. (23). We recruited four twin pairs, discordant for obesity (obese twin BMI > 30kg/m^2) with a sustained multi-year BMI difference of ≥5.5 kg/m^2 (n=1 MZ; 3 DZ pairs; Fig. 1A). Fecal samples were collected from each twin, frozen immediately after they were produced, and stored at −80°C. Each fecal sample was introduced, via a single oral gavage, into a group of 8–9-week-old adult male germ-free C57BL/6J mice (one gnotobiotic isolator/microbiota sample; each recipient mouse individually caged within the isolator; n=3–4 mice/donor microbiota sample/experiment; n=1–5 independent experiments/microbiota). All recipient mice were fed a commercial, sterilized mouse chow that was low in fat (4% by weight) and high in plant polysaccharides (LF/HPP), *ad libitum* (23). Fecal pellets were obtained from each mouse 1, 3, 7, 10 and 15 days post colonization (dpc); and for more prolonged experiments on days 17, 22, 24, 29, and 35.

Unweighted UniFrac-based comparisons of bacterial 16S rRNA datasets generated from the input human donor microbiota, from fecal samples collected from gnotobiotic mice, and from different locations along the length of the mouse gut at the time of sacrifice (table S1A), plus comparisons of the representation of genes with assignable enzyme commission numbers (ECs) in human fecal and mouse cecal microbiomes (defined by shotgun sequencing), disclosed that transplant recipients efficiently and reproducibly captured the taxonomic features of their human donor's microbiota and the functions encoded by the donor's microbiome [see Fig. 1B, fig. S1A–D, fig. S2, table S1B, table S2A–D, plus (23)]. The 16S rRNA datasets allowed us to identify bacterial taxa that differentiate gnotobiotic mice harboring gut communities transplanted from all lean versus all obese co-twins [analysis of variance using Benjamini-Hochberg correction for multiple hypotheses; table S3; see (23) for further details].

Reproducible transmission of donor body composition phenotypes

Quantitative magnetic resonance (qMR) analysis was used to assess the body composition of transplant recipients 1d, 15d, and in the case of longer experiments, 8d, 22d, 29d and 35d after transplantation. The increased adiposity phenotype of each obese twin in a discordant twin pair was transmissible: the change in adipose mass of mice that received an obese co-twin's fecal microbiota was significantly greater than the change in animals receiving her lean twin's gut community within a given experiment, and was reproducible across experiments ($p \leq 0.001$, one-tailed unpaired Student's *t*-test; n=103 mice phenotyped; Fig. 1C–E). Epididymal fat pad weights were also significantly higher in mice colonized with gut communities from obese twins ($p \leq 0.05$, one-tailed unpaired Student's *t*-test). These differences in adiposity were not associated with statistically significant differences in daily chow consumption (measured on days 1, 8 and 15 after gavage and weekly thereafter for longer experiments), or with appreciably greater inflammatory responses in recipients of obese compared to lean co-twin fecal microbiota as judged by FACS analysis of the $CD4^+$ and $CD8^+$ T cell compartments in spleen, mesenteric lymph nodes, small intestine or colon [see (23) for details].

Functional differences between transplanted microbial communities

Fecal samples collected from gnotobiotic mice were used to prepare RNA for microbial RNA-Seq characterization of the transplanted microbial communities' meta-transcriptomes (table S1C). Transcripts were mapped to a database of sequenced human gut bacterial genomes and assigned to KEGG ECs [see ref. (23)]. Significant differences and distinguishing characteristics were defined using ShotgunFunctionalizeR, which is based on

a Poisson model (24) (see table S4 and table S5 for ECs and KEGG level 2 pathways, respectively). Transcripts encoding 305 KEGG ECs were differentially expressed between mice harboring microbiomes transplanted from lean or obese donors (ShotgunFunctionalizeR, AIC<5,000; $p \leq 10^{-30}$).

Mice harboring the transplanted microbiomes from the obese twins exhibited higher expression of microbial genes involved in detoxification and stress responses, in biosynthesis of cobalamin, metabolism of essential amino acids (phenylalanine, lysine, valine, leucine and isoleucine) and nonessential amino acids (arginine, cysteine and tyrosine), and in the pentose phosphate pathway (fig. S3A, B; table S4B–G and table S5). Follow-up targeted MS/MS-based analysis of amino acids in sera obtained at the time of sacrifice demonstrated significant increases in branched chain amino acids (BCAA; Val and Leu/Ile), as well as other amino acids (Met, Ser and Gly), plus trends to increase Phe, Tyr and Ala, in recipients of microbiota from obese compared with lean co-twins in discordant twin pairs DZ1 and MZ4 (tables S1D, S6A). These specific amino acids, as well as the magnitude of their differences are remarkably similar to elevations in BCAA and related amino acids reported in obese, insulin-resistant versus lean, insulin-sensitive humans (25). This finding suggested that the gut microbiota from obese subjects could influence metabolites that characterize the obese state.

In contrast, the transplanted microbiomes from lean co-twins exhibited higher expression of genes involved in (i) digestion of plant-derived polysaccharides [e.g., alpha-glucuronidase (EC 3.2.1.139), alpha-L-arabinofuranosidase (EC 3.2.1.55)], and (ii) fermentation to butyrate [acetyl-CoA C-acetyltransferase (EC 2.3.1.9), 3-hydroxybutyryl-CoA dehydrogenase (EC 1.1.1.157), 3-hydroxybutyryl-CoA dehydratase (EC 4.2.1.55), butyryl-CoA dehydrogenase (EC 1.3.99.2)] (fig. S3C, D), and propionate [succinate dehydrogenase (EC 1.3.99.1), phosphoenolpyruvate carboxykinase (EC 4.1.1.32), methylmalonyl-CoA mutase (EC 5.4.99.2)] (table S4A). Follow up gas chromatography-mass spectrometry (GC/MS) of cecal contents confirmed that levels of butyrate and propionate were significantly increased, and that levels of several mono- and disaccharides significantly decreased in animals colonized with lean compared to obese co-twin gut communities ($p \leq 0.05$, unpaired Student's *t*-test, fig. S4A, B, table S6B). Procrustes analysis, using a Hellinger distance matrix (26), revealed significant correlations between taxonomic structure (97%ID OTU-level bacterial phylotypes in fecal samples), transcriptional profiles (EC representation in fecal mRNA populations), and metabolic profiles (GC/MS of cecal samples), with separation of groups based on donor microbiota and BMI (fig. S5; Mantel test, $p \leq 0.001$).

These results suggest that in this diet context, transplanted microbiota from lean co-twins had a greater capacity to breakdown and ferment polysaccharides than the microbiota of their obese co-twins. Previous reports have shown that increased microbial fermentation of non-digestible starches is associated with decreased body weight and decreased adiposity in conventionally-raised mice that harbor a mouse microbiota [e.g. refs. (27–29)].

Phenotypes produced by bacterial culture collections

We followed up these studies of transplanted, intact, uncultured donor communities with a set of experiments involving culture collections produced from the fecal microbiota of one of the discordant twin pairs. Our goal was to determine whether cultured bacterial members of the co-twins' microbiota could transmit the discordant adiposity phenotypes and associated distinctive microbiota metabolic profiles when transplanted into gnotobiotic mouse recipients who received the LF/HPP chow diet. Collections of cultured anaerobic bacteria were generated from each co-twin in DZ pair 1 and subsequently introduced into separate groups of 8-week-old germ-free male C57BL/6J mice (n=5 independent

experiments; 4–6 recipient mice/culture collection/experiment). The culture collections stabilized in the guts of recipient mice within 3 d after their introduction [see ref. (23), fig. S6A–E and table S7 for documentation of the efficient and reproducible capture of cultured taxa and their encoded gene functions between groups of recipient mice].

As in the case of uncultured communities, we observed a significantly greater increase in adiposity in recipients of the obese twin's culture collection compared to the lean co-twin's culture collection ($p \leq 0.02$, one-tailed unpaired Student's *t*-test; Fig. 2A, B). Nontargeted GC/MS showed that the metabolic profiles generated by the transplanted culture collections clustered with the profiles produced by the corresponding intact uncultured communities (fig. S6E). In addition, the fecal biomass of recipients of the culture collection from the lean twin was significantly greater than the fecal biomass of mice receiving the culture collection from her obese sibling: these differences were manifest within 7 d ($p \leq 0.0001$, two-way ANOVA; fig. S7A).

Co-housing Ob and Ln animals prevents an increased adiposity phenotype

Because mice are coprophagic, the potential for transfer of gut microbiota through the fecal-oral route is high. Therefore, we used co-housing to determine whether exposure of a mouse harboring a culture collection from the lean twin could prevent development of the increased adiposity phenotype and microbiome-associated metabolic profile of a cagemate colonized with the culture collection from her obese co-twin, or vice versa. Five days after gavage, when each of the inoculated microbial consortia had stabilized in the guts of recipient animals, a mouse with the lean co-twin's culture collection was co-housed with a mouse with the obese co-twin's culture collection (abbreviated Ln^{ch} and Ob^{ch}, respectively). Control groups consisted of cages of dually-housed recipients of the lean twin culture collection and dually-housed recipients of the obese co-twin's culture collection (n=3–5 cages/housing configuration/experiment; n=4 independent experiments; each housing configuration in each experiment placed in separate gnotobiotic isolators; Fig. 2A). All mice were 8-week-old C57BL/6J males. All were fed the same LF/HPP chow *ad libitum* that was used for transplants involving the corresponding uncultured communities. Bedding was changed prior to initiation of co-housing. Fecal samples were collected from all recipients 1, 2, 3, 5, 6, 7, 8, 10 and 15 days following gavage. Body composition was measured by qMR 1 and 5 days after gavage, and after 10 days of co-housing.

Ob^{ch} mice exhibited a significantly lower increase in adiposity compared to control Ob animals that had never been exposed to mice harboring the lean co-twin's culture collection ($p \leq 0.05$, one-tailed unpaired Student's *t*-test). Moreover, the adiposity of these Ob^{ch} animals was not significantly different from Ln controls ($p > 0.05$, one-tailed unpaired Student's *t*-test; Fig. 2B). In addition, exposure to Ob^{ch} animals did not produce a significant effect on the adiposity of Ln^{ch} mice: their adiposity phenotypes and fecal biomass were indistinguishable from dually-housed Ln controls (Fig. 2B; fig. S7B, C). Co-housing caused the cecal metabolic profile of Ob^{ch} mice to assume features of Ln^{ch} and control Ln animals, including higher levels (compared to dually-housed Ob controls) of propionate and butyrate, and lower levels of cecal mono- and disaccharides as well as branched chain and aromatic amino acids (Fig. 2C, D; fig. S8).

Principal coordinates analysis of unweighted UniFrac distances revealed that the fecal microbiota of Ob^{ch} mice were re-configured so that they came to resemble the microbiota of Ln^{ch} cagemates. In contrast, the microbiota of the Ln^{ch} cagemates remained stable (fig. S9A–C). We performed a follow-up analysis to identify species-level taxa that had infiltrated into and/or had been displaced from the guts of mice harboring the Ln and Ob culture collections. We did so by characterizing the direction and success of invasion.

Microbial SourceTracker estimates the Bayesian probability (*P*) for every species-level taxon or 97%ID OTU to be derived from each of a set of source communities (30). The fecal microbiota of Ln or Ob controls sampled 5 days after colonization were used as source communities to determine the direction of invasion. The fecal communities belonging to each Ln^{ch} and Ob^{ch} mouse were then traced to these sources. We defined the direction of invasion for these bacterial taxa, by calculating the log odds ratio of the probability of a Ln origin (*PLn*) or an Ob origin (*POb*) for each species-level taxon or 97%ID OTU, *i*:

$$\log_2[PLn_i/POb_i]$$

A positive log odds ratio indicated that a species or 97%ID OTU was derived from a Ln source, while a negative log odds ratio indicated an Ob source. An invasion score was calculated to quantify the success of invasion of each species or 97%ID OTU, *i*, into each co-housing group, *j*:

$$Invasion\ Score_{ij} = \log_2[\overline{A_{ij}}/\overline{B_{ij}}]$$

where $\overline{A_{ij}}$ is the average relative abundance of taxon *i* in all fecal samples collected from group *j* after cohousing, and $\overline{B_{ij}}$ is its relative abundance in all samples taken from that group before cohousing.

The observed mean of the distribution of invasion scores for Ob^{ch} animals was significantly higher than that for dually-housed Ob-Ob controls ($p \leq 0.0005$, Welch's two-sample *t*-test; fig. S10A). This was not the case for Ln^{ch} animals when compared to dually housed Ln-Ln controls ($p > 0.05$), suggesting that there was significant invasion of components of the Ln^{ch} microbiota into the microbiota of Ob^{ch} cagemates, but not vice versa. To quantify invasion further, we used the mean and standard deviation of the null distribution of invasion scores (defined as the scores from recipients of the Ln or Ob microbiota that had never been co-housed with each other) to calculate a z-value and a Benjamini-Hochberg adjusted *p*-value for the invasion score of each species in Ln^{ch} and Ob^{ch} mice. We conservatively defined a taxon as a successful invader if it (i) had a Benjamini-Hochberg adjusted $p \leq 0.05$, (ii) was represented in ≥75% of Ob^{ch} or Ln^{ch} mice when sampled 7 and 10 d after initiation of co-housing, and (iii) had a relative abundance of ≤0.05% before cohousing and ≥0.5% in the fecal microbiota at the time of sacrifice. We defined a taxon that was displaced from an animal's microbiota upon co-housing as having a relative abundance ≥1% in Ln^{ch} or Ob^{ch} mice before they were co-housed and a relative abundance <0.5% after co-housing.

Fig. 2E and table S8A provide information about the direction and success of invasion. The most successful Ln^{ch} invaders of the Ob^{ch} microbiota were members of the Bacteroidetes (rank order of their invasion scores: *Bacteroides cellulosilyticus*, *Bacteroides uniformis*, *Bacteroides vulgatus*, *Bacteroides thetaiotaomicron*, *Bacteroides caccae, Alistipes putredinis* and *Parabacteroides merdae)*. Invasiveness exhibited specificity at the 97%ID OTU level (fig. S11). In contrast, co-housing did not result in significant invasion of Ln^{ch} intestines with members of the Ob^{ch} microbiota.

In macroecosystems, successful invaders are often more likely to become established if they are from divergent taxa that do not share a niche with members of the native entrenched community (31, 32). We used the Net Relatedness Index (NRI; (33)) to show that Ln and Ob communities have different phylogenetic structures, and that the patterns of phylogenetic clustering and dispersion of Ob, but not Ln microbiota, change as a consequence of co-housing. Specifically fecal Ln, Ln^{ch} and Ob^{ch} communities had a negative NRI, which

indicates that the community is more phylogenetically dispersed. Furthermore, the fecal communities of Ln^{ch} and Ob^{ch} animals had significantly more shared branch length with each other after co-housing compared to before co-housing [see (23)] for a description of calculations and interpretation plus fig. S9E and fig. S12). Together, these patterns of phylogenetic over-dispersion and increased shared branch length in cohoused Ln^{ch} and Ob^{ch} animals, led us to hypothesize that Bacteroides in the Ln^{ch} community were efficient invaders of Ob^{ch} communities because they were able to occupy un-occupied niches in Ob^{ch} intestines. Interestingly, increased representation of Bacteroidetes has been documented in several independent studies of the gut microbiota of conventionally-raised lean mice compared to mice with genetic- or diet-induced obesity (34, 35).

Control experiments involving co-housing a germ-free (GF^{ch}) mouse with an Ob mouse 5d after transplantation of the complete culture collection from the obese co-twin, demonstrated effective transmission of the Ob adiposity phenotype to the GF cagemate (defined by epididymal fat pad weight as a percentage of total body weight; $p > 0.05$, comparing $GF^{ch\text{-}Ob}$ and $Ob^{ch\text{-}GF}$ cagemates with a two-tailed unpaired Student's *t*-test). The adiposity of the $GF^{ch\text{-}Ob}$ cagemate was significantly greater compared to GF-GF controls [1.4±0.1% ($Ob^{ch\text{-}GF}$); 1.4±0.05% ($GF^{ch\text{-}Ob}$); 1.5±0.05% (Ob-Ob controls) versus 0.8±0.06% (GF-GF controls); $p<10^{-4}$, two-tailed unpaired Student's *t*-test between $GF^{ch\text{-}Ob}$ and GF-GF controls; n=6 GF-GF; 8 Ob-Ob; 10 $GF^{ch\text{-}Ob}$-$Ob^{ch\text{-}GF}$)].

In separate experiments, we co-housed two GF animals together with one Ln and one Ob animal, 5d after colonization of Ln and Ob mice (repeated in three separate cages, each cage in a separate isolator). As with previous experiments, bedding was changed prior to initiation of co-housing. The GF 'bystanders' did not develop increased adiposity phenotypes, and manifested cecal metabolic profiles and fecal biomass characteristics of their Ln^{ch} cagemates and Ln controls (Fig. 2B–E, fig. S7F). In the initial phase of co-housing (days 1–2), the microbiota of GF^{ch} mice in each cage resembled that of non-co-housed Ob-Ob controls (fig. S9D). By the next day, the microbiota of each ex-GF^{ch} had undergone a dramatic change in composition, with 94.8 ± 0.4% of taxa now derived from their Ln^{ch} cagemate (defined by SourceTracker; see table S8A for log odds ratio scores). The most prominent invaders were the same prominent invaders from the Ln^{ch} microbiota described above (i.e., all of the *Bacteroides*; Fig. 2E). We concluded that these Ln-derived taxa had greater fitness in the guts of C57BL/6J mice consuming this diet, and had a 'dominant-negative' effect on host adiposity.

Changes in the cecal meta-transcriptome and metabolome of Ob^{ch} animals

Cecal samples collected at the time of sacrifice from Ln^{ch}, Ob^{ch} and control Ob and Ln animals were subjected to microbial RNA-Seq. Reads were assigned to ECs as above, and Euclidean distances were calculated from the EC matrix. The results revealed that the meta-transcriptomes of Ob^{ch} animals were significantly more similar to those of their Ln^{ch} cagemates and Ln controls than to Ob controls, consistent with a functional transformation of the Ob^{ch} microbiota to a lean-like state as a consequence of invasion of the Ln taxa (fig. S13; $p \leq 0.0001$ as measured by a one-way ANOVA, with Holm-Šidák's correction for multiple hypotheses). The majority (55.9%) of ECs that were enriched in the cecal meta-transcriptomes of Ob^{ch} mice compared to dually-housed Ob-Ob controls were also significantly enriched in dually-housed Ln-Ln versus Ob-Ob controls, including ECs that participate in carbohydrate metabolism and protein degradation. The latter encompassed five enzymes involved in the KEGG pathway for degradation of the BCAA valine, leucine and isoleucine (transcripts encoding EC1.2.4.4; EC 2.6.1.42; EC5.1.99.1 and EC6.4.1.3 which map to the genomes of invading members of the *Bacteroides*, and EC.4.2.1.17 which maps to members of Clostridiaceae; table S9). The increased expression of genes involved in

BCAA degradation is consistent with the reduced cecal levels of BCAA observed in Ob^{ch} versus Ob-Ob controls (fig. S8), and suggests that invasion by *Bacteroides* increases the efficiency of BCAA degradation in the gut, reducing production of BCAA and related metabolites by the microbiome and contributing to decreased circulating levels of BCAA in the host. As with transplanted intact uncultured microbiota from the discordant twin pairs, targeted MS/MS analysis confirmed that Ob-Ob controls had a global increase in serum levels of BCAAs as well as higher levels of Met, Ser, Gly, Phe, Tyr and Ala compared to Ln-Ln controls (table S10; $p \leq 0.05$, matched one-way ANOVA). However, after a 10 d co-housing, Ob^{ch} animals did not exhibit a statistically significant reduction in serum BCAA levels compared to Ob-Ob controls, although levels in Ln^{ch} cagemates were significantly lower than in Ob-Ob controls and not different from Ln controls (table S10). More complete understanding of the contributions of the gut microbial community to Ob-associated metabolic phenotypes will require detailed, long-term, time series studies of microbial and host transcriptomes and metabolomes.

Fig. 3A summarizes significant correlations between cecal metabolite levels and bacterial species represented in the microbiota of Ob-Ob, Ln-Ln, Ln^{ch}, and Ob^{ch} and GF^{ch} mice consuming the LF/HPP diet (defined by asymptotic *p*-values for all Spearman's correlations, corrected for multiple hypotheses using the Benjamini-Hochberg procedure). For example, BCAA and the products of amino acid metabolism were positively correlated with *Clostridium hathewayi* (Fig. 3A). This member of the Firmicutes represented an average of 2.54%of the Ob fecal microbiota prior to co-housing; its relative abundance was significantly reduced in Ob^{ch} animals and it was not able to successfully invade the microbiota of Ln^{ch} cagemates (Fig. 2E, Fig. 3A, table S8A).

Three members of the Bacteroidetes, *Bacteroides uniformis*, *Parabacteroides merdae*, and *Alistipes putredinis*, which were prominent invaders of the Ob^{ch} gut, positively correlated with cecal acetate, propionate and butyrate levels. Whereas members of these species generate acetate and propionate, their ability to produce butyrate has not been reported. Their positive association with butyrate levels could be due to interspecies acetate cross-feeding with butyrate-producing taxa (36, 37). The negative correlation between adiposity and cecal butyrate and propionate concentrations in Ln^{ch}, Ob^{ch}, and GF^{ch} microbiota ($r = -0.49$ and -0.45 respectively, $p \leq 0.05$) is consistent with previous studies claiming a role for these SCFAs in influencing host energy balance (38, 39).

The gut microbiota impacts the composition and relative abundance of bile acids species through a variety of metabolic transformations (40, 41). Ultra performance liquid chromatography-mass spectrometry (UPLC-MS) analysis of 37 bile acid species in cecal samples obtained from Ln-Ln, Ob-Ob, Ob^{ch}, and Ln^{ch} mice revealed significantly lower levels of eight bile acids in Ob-Ob compared to Ln-Ln controls (Fig. 3B). Co-housing rescued these differences, with Ob^{ch} mice having bile acid profiles that were more similar to Ln-Ln than to Ob-Ob controls, and not significantly different from Ln^{ch} cagemates (n=5–6 mice/group; see table S11 for all bile acids measured that exhibit significant differences between Ob-Ob and Ln-Ln controls).

Bile acids can have direct metabolic effects on the host via the nuclear farnesoid X receptor (FXR) (42). Intestinal FXR mediates intestinal fibroblast growth factor 15 (*Fgf15)* production. Fgf15, secreted by the gut epithelium and delivered to hepatocytes via the portal circulation, acts through fibroblast growth factor receptor 4 (*Fgfr4*) to inhibit expression of the rate-limiting enzyme in bile acid biosynthesis, cholesterol 7-alpha-hydroxylase (*Cyp7a1*) [Fig. 3C–F; (43)]. Engineered FXR deficiency in leptin-deficient mice protects against obesity and improves insulin sensitivity (42). Over-expression of *Cyp7a1* in the livers of transgenic mice also prevents diet-induced obesity and insulin resistance (44). Sequestering

bile acids with the drug colesevelam lowers blood sugar in humans with type 2 diabetes (45). qRT-PCR analysis disclosed that compared to Ln-Ln animals, Ob-Ob mice have increased FXR and *Fgf15* mRNA levels in their distal small intestine (ileum) and decreased hepatic *Cyp7a1* expression. Ob^{ch} mice have expression profiles that are not significantly different from Ln-Ln controls (or Ln^{ch}; Fig. 3C–E). Differences in bile acid metabolism, in addition to the documented differences in carbohydrate fermentation by Ob compared to Ln microbial communities highlight some of the mechanisms that could contribute to the observed microbiota-mediated effects on body composition.

Taxa-specific effects on body composition and metabotype

We subsequently colonized GF mice with a consortium of 39 sequenced taxa (97%ID OTUs) from the lean co-twin's culture collection; 22 OTUs from *Bacteroides*, including *B. cellulosilyticus, B. vulgatus, B. thetaiotaomicron, B. caccae, B. ovatus*; 11 OTUs from *Ruminococcaceae* (one of the four family-level taxa that discriminate lean from obese), and six strains of *Collinsella aerofaciens* (see table S12 for features of their sequenced genomes). Five days after colonization with the 39 taxa, these Ln^{39} mice were co-housed with Ob mice. Control groups consisted of dually housed Ln-Ln and dually-housed Ob-Ob animals (fig. S14A; n=5 cages of co-housed animals/group; 2 independent experiments). Mice harboring the 39-member consortium ($Ln39^{ch}$) when co-housed with Ob (Ob^{chLn39}) animals remained lean (fig. S14B). However, $Ln39^{ch}$ animals were not able to confer protection against an increase in adiposity of their Ob^{ch} cagemates, nor did they exhibit a significant increase in their cecal butyrate levels (fig. S14C, fig. S7D, E). Even though some species like *B. cellulosilyticus* and *B. vulgatus* from the $Ln39^{ch}$ microbiota exhibited significant invasion into the microbiota of $Ob^{ch\text{-}Ln39}$ cagemates, there was an overall decrease in invasion efficiency for members of the Ln39 consortia compared to those in the complete Ln culture collection [the mean of the distribution of invasion scores for the $Ob^{ch\text{-}Ln39}$ microbiota was not significantly different from Ob-Ob controls ($p > 0.05$, Welch's Two Sample *t*-test; fig. S10B, table S8B)]. These findings illustrate how invasiveness and adiposity are dependent upon community context.

Diet-specific effects

To define the effects of diet on Ln and Ob microbiota-mediated transmission of body composition and metabolic phenotypes, we constructed a diet made with foods that characterize diets representing the lower tertile of consumption of saturated fats and the upper tertile of consumption of fruits and vegetables reported in one day recalls in the USA National Health and Nutrition Examination Survey (NHANES) during the period 2003–2008 [table S13; (23)]. Mice fed this low saturated fat, high fruits and vegetables (LoSF/HiFV, ~33% kcal of fat/100g) NHANES-based diet were colonized with either the Ln or Ob human culture collections and subsequently co-housed. Dually-housed Ln-Ln and Ob-Ob animals served as reference controls (n=3–5 cages/housing configuration; 2 independent experiments). Ob-Ob cagemates consuming the LoSF/HiFV diet had significantly increased body mass compared to Ln-Ln cagemates, reflecting a significant increase in both adipose and lean body mass (one-way unpaired Student's *t*-test; $p \leq 0.001$; Fig. 4A, B; table S14). Co-housing prevented development of an Ob body composition phenotype in Ob^{ch} animals (Fig. 4A, B).

16S rRNA analysis of fecal samples collected 1–8,10,12 and 14 d after gavage of the culture collections revealed that this rescue was accompanied by invasion of taxa from Ln^{ch} to Ob^{ch} cagemates ($p \leq 10^{-6}$; Welch's two sample *t*-test comparing the mean of the distributions of invasion scores between Ob-Ob controls and Ob^{ch} animals) with the most invasive species being members of *Bacteroides* (i.e., *B. uniformis, B. vulgatus* and *B. cellulosilyticus;* Fig. 5,

fig. S15A–C, fig. S10C). These species were also successful invaders in mice fed the LF/HPP diet (Fig. 2E). As was the case with the LF/HPP mouse chow, fecal samples collected from Ln-Ln controls, and from Ln^{ch} and Ob^{ch} animals fed the human (NHANES-based) LoSF/HiFV diet had significantly greater microbial biomass compared to Ob-Ob controls (two-way ANOVA, $p \leq 0.001$ after Holm-Šidák's correction for multiple hypothesis). Moreover, fecal microbial biomass in Ob^{ch} and Ln^{ch} animals was not significantly different (data not shown).

Fig. 4C summarizes significant correlations between cecal metabolites and cecal bacterial taxa in mice fed a LoSF/HiFV diet. As in mice fed a LF/HPP diet, the invasive species *B. uniformis* and *B. vulgatus* were significantly and positively correlated with increased cecal propionate levels in Ln-Ln, Ob^{ch} and Ln^{ch} animals compared to Ob-Ob controls.

Obesity-related insulin resistance has been associated with broad-scale accumulation of acylcarnitines in skeletal muscle (46, 47). Maneuvers that resolve the acylcarnitine accumulation in muscle, including knockout of the malonylCoA decarboxylase gene (*Mlycd*) or overexpression of carnitine acyltransferase (*Crat*) also resolve the insulin resistance phenotype in mice (47, 48). Therefore, we used targeted MS/MS to measure 60 acylcarnitine species (C2 to C22) in liver, skeletal muscle and serum (tables S15A–C). When fed the LF/HPP mouse chow (4% fat by weight), Ob-Ob animals had significantly higher levels of hepatic short-chain acylcarnitines (C2, C4:C4i and C4-OH) compared to Ln-Ln mice (fig. S16; two-way ANOVA after Holm- Šidák's correction). The differences in short-chain acylcarnitines were rescued in Ob^{ch} animals, which resembled Ln-Ln controls (n=5 animals/treatment group).

Ob-Ob controls fed the LoSF/HiFV diet (33% fat by weight) also had clear increases in accumulation of a group of even-, long-chain acylcarnitines (C14, C14:1, C16, C16:1, C18, C18:1, C18:2) in their liver and skeletal muscle compared to Ln-Ln controls (MANOVA, $p \leq 0.001$; n=3–6 animals/treatment group). Co-housing Ln and Ob animals rescued this metabolic phenotype in the skeletal muscle and liver (and cecum) of Ob^{ch} mice (i.e., there was no statistically significant difference compared to Ln-Ln controls; Fig. 6, fig. S16, table S15). There were no significant differences in accumulation of these acylcarnitines in the plasma of Ob-Ob, Ln-Ln and co-housed animals (table S15B, C) suggesting that the gut microbiome influences systemic lipid metabolism.

Since these findings raised the possibility that the Ob microbiome is capable of conferring muscle insulin resistance at least in the context of a human (LoSF/HiFV) diet, we subjected Ob-Ob and Ln-Ln animals to a glucose tolerance test 15 d after colonization with their human donor's gut culture collections. An increase in serum glucose concentration was observed 15 min after intraperitoneal injection of glucose in Ob-Ob animals (mean ± SEM: 338.5±11.07 mg/dL in Ob-Ob animals, versus 304.6±17.78 mg/dL in Ln-Ln animals; $p = 0.06$, unpaired Student's *t*-test; n=11-10 animals/group). No significant differences in serum insulin concentrations between these groups were documented at 30 min after glucose was administered, nor did we observe significant differences in insulin signaling in liver and skeletal muscle, defined by levels of immunoreactive Akt phosphorylated at Thr308 and the Akt substrate AS160 phosphorylated at Thr642 measured 3 min following an insulin bolus (23). We concluded that the elevation in skeletal muscle long-chain acylcarnitines observed in mice colonized for just 15 days with an Ob culture collection and consuming the LoSF/HiFV diet is associated with mild glucose intolerance, and may be an early manifestation of the pathobiologic effects of obese microbiota on host physiology and metabolism. More complete time course studies will be required to test if this lesion in glucose homeostasis will evolve into full-fledged insulin resistance with longer exposure to Ob microbiota.

To determine if the effects exerted by diet on the invasive potential of members from the Ln microbiota were specific to the culture collections prepared from members of discordant twin pair 1, or robust to other Ln co-twin microbiota, we fed the LoSF/HiFV diet to mice colonized with intact uncultured fecal microbiota from members of discordant twin pair 2. Co-housing experiments performed using the same experimental design described above revealed significant invasion of the communities of Ob^{ch} animals by bacterial species from their Ln^{ch} cagemates, most notably a member of the Bacteroidetes: *Parabacteroides distasonis* (figs. S10D, fig. S17A).

In follow-up experiments, separate groups of germ-free mice colonized with intact uncultured microbiota from discordant twin-pair 2 were fed a second NHANES-based diet made with foods that characterize USA diets representing the upper rather than lower tertile of consumption of saturated fats, and the lower rather than upper tertile of consumption of fruits and vegetables (abbreviated HiSF/LoFV; 44% fat by weight). Significant differences in body composition were documented between Ob-Ob and Ln-Ln mice on this diet. However, co-housing of Ln and Ob mice failed to attenuate or block development of an increased body mass phenotype in Ob^{ch} cagemates (n=5–11 animals/housing configuration; Fig. 4D, E). Remarkably, there was a lack of significant invasion of members of the Ln^{ch} microbiota into the guts of Ob^{ch} cagemates (fig. S10E, fig. S17B). Moreover, if biased fecal pellet consumption was the underlying mechanism leading to invasion of members of the Ln microbiota into the guts of Ob^{ch} mice in the co-housing experiments, it would have to be diet- and microbiota-dependent. Together, these results emphasize the strong microbiota-by-diet interactions that underlie invasion, and illustrate how a diet high in saturated fats and low fruits and vegetables can select against human gut bacterial taxa associated with leanness.

Prospectus

The findings described above provide a starting point for future studies that systematically test the effects of specified diet ingredients on microbiota-associated body composition and metabolic phenotypes (e.g., components that when added or subtracted restore invasiveness of specific members of the microbiota in the context of the HiSF/LoFV diet). A benefit of using the approach described in this report is that the target human population embodying a phenotype of interest is integrated into the animal model through selection of gut microbiota representative of that population and diets representative of their patterns of food consumption. Our finding that culture collections generated from human microbiota samples can transmit donor phenotypes of interest (body composition, metabotypes) has a number of implications. If these derived culture collections can transmit a phenotype, the stage is set for studies designed to determine which culturable components of a given person's gut community are responsible. These tests can take the form of co-housing experiments where mice containing culture collections from donors with different phenotypes are co-housed and used to determine whether invasion by components of one community into another transforms the cagemate's phenotype and, correspondingly, the properties of the human microbial communities they harbor. Sequenced culture collections generated from human gut microbiota donors also provide an opportunity to model and further address basic issues such as the determinants of invasiveness including the mechanisms by which invasion is impacted by diet composition, as well as the mechanisms by which invading components impact microbial and host metabolism. This issue is important for identifying next generation probiotics, prebiotics or a combination of the two (synbiotics). Moreover, the ability to generate a culture collection, from an individual, whose composition is resolved to the gene level, whose properties can be validated in preclinical models, and whose 'manufacture' is reproducible, may provide a safer and more sustainable alternative to fecal transplants for microbiome-directed therapeutics (18, 49).

Supplementary Material

Refer to Web version on PubMed Central for supplementary material.

Acknowledgments

We thank David O'Donnell, Maria Karlsson, Sabrina Wagoner, Janaki Guruge, Robin Chamberland, Marty Meier, and Su Deng for superb technical assistance, Philip Ahern for help with FACS analysis, Deborah Hopper and Stacey Marion for their contributions to the recruitment of discordant twins from the MOAFTS cohort and for obtaining fecal samples for the present study, Ilia Halatchev for help in performing diet experiments, plus Alejandro Reyes and Nathan McNulty for many helpful suggestions. Stephan Baumann and Steven Fischer (Agilent Technologies, Santa Clara, CA) provided technical support for some of the metabolomics analyses including a gift of the Fiehn metabolite library. This work was supported in part by grants from the NIH (DK078669, DK70977, P30-AG028716 and DK58398), the Crohn's and Colitis Foundation of America, plus Kraft Foods and Mondelez International. Bacterial 16S rRNA pyrosequencing reads have been deposited in EBI (accession number), as have shotgun pyrosequencing datasets from cecal community DNA (accession number) and draft microbial genome assemblies. RNA-Seq datasets can be found in the Gene Expression Omnibus (accession number).

References and Notes

1. Eckburg PB, et al. Diversity of the human intestinal microbial flora. Science. 2005; 308:1635. [PubMed: 15831718]
2. Turnbaugh PJ, et al. A core gut microbiome in obese and lean twins. Nature. 2009; 457:480. [PubMed: 19043404]
3. Costello EK, et al. Bacterial community variation in human body habitats across space and time. Science. 2009; 326:1694. [PubMed: 19892944]
4. Qin J, et al. A human gut microbial gene catalogue established by metagenomic sequencing. Nature. 2010; 464:59. [PubMed: 20203603]
5. Ravel J, et al. Vaginal microbiome of reproductive-age women. Proc Natl Acad Sci U S A. 2011; 108:4680. [PubMed: 20534435]
6. Gajer P, et al. Temporal dynamics of the human vaginal microbiota. Sci Transl Med. 2012; 4:132ra52.
7. Yatsunenko T, et al. Human gut microbiome viewed across age and geography. Nature. 2012; 486:222. [PubMed: 22699611]
8. HMP Consortium. Structure, function and diversity of the healthy human microbiome. Nature. 2012; 486:207. [PubMed: 22699609]
9. Faust K, et al. Microbial Co-occurrence Relationships in the Human Microbiome. PLoS Comput Biol. 2012; 8:e1002606. [PubMed: 22807668]
10. Dominguez-Bello MG, et al. Delivery mode shapes the acquisition and structure of the initial microbiota across multiple body habitats in newborns. Proc Natl Acad Sci U S A. 2010; 107:11971. [PubMed: 20566857]
11. Koenig JE, et al. Succession of microbial consortia in the developing infant gut microbiome. Proc Natl Acad Sci U S A. 2011; 108:4578. [PubMed: 20668239]
12. Greenblum S, Turnbaugh PJ, Borenstein E. Metagenomic systems biology of the human gut microbiome reveals topological shifts associated with obesity and inflammatory bowel disease. Proc Natl Acad Sci U S A. 2012; 109:594. [PubMed: 22184244]
13. Zupancic ML, et al. Analysis of the gut microbiota in the old order Amish and its relation to the metabolic syndrome. PLoS One. 2012; 7:e43052. [PubMed: 22905200]
14. Duncan SH, et al. Human colonic microbiota associated with diet, obesity and weight loss. Int J Obes (Lond). 2008; 32:1720. [PubMed: 18779823]
15. Schwiertz A, et al. Microbiota and SCFA in lean and overweight healthy subjects. Obesity (Silver Spring). 2010; 18:190. [PubMed: 19498350]
16. Santacruz A, et al. Gut microbiota composition is associated with body weight, weight gain and biochemical parameters in pregnant women. Br J Nutr. 2010; 104:83. [PubMed: 20205964]

17. Jumpertz R, et al. Energy-balance studies reveal associations between gut microbes, caloric load, and nutrient absorption in humans. Am J Clin Nutr. 2011; 94:58. [PubMed: 21543530]
18. Vrieze A, et al. Transfer of Intestinal Microbiota from Lean Donors Increases Insulin Sensitivity in Subjects with Metabolic Syndrome. Gastroenterology. 2012
19. Hakala P, Rissanen A, Koskenvuo M, Kaprio J, Ronnemaa T. Environmental factors in the development of obesity in identical twins. Int J Obes Relat Metab Disord. 1999; 23:746. [PubMed: 10454109]
20. Rissanen A, et al. Acquired preference especially for dietary fat and obesity: a study of weight-discordant monozygotic twin pairs. Int J Obes Relat Metab Disord. 2002; 26:973. [PubMed: 12080452]
21. Duncan AE, et al. Genetic and environmental contributions to BMI in adolescent and young adult women. Obesity (Silver Spring). 2009; 17:1040. [PubMed: 19165159]
22. Waldron M, Bucholz KK, Lynskey MT, Madden PA, Heath AC. Alcoholism and timing of separation in parents: findings in a midwestern birth cohort. J Stud Alcohol Drugs. 2013; 74:337. [PubMed: 23384382]
23. Materials and methods are available as supplementary material on *Science* Online.
24. Kristiansson E, Hugenholtz P, Dalevi D. ShotgunFunctionalizeR: an R-package for functional comparison of metagenomes. Bioinformatics. 2009; 25:2737. [PubMed: 19696045]
25. Newgard CB, et al. A branched-chain amino acid-related metabolic signature that differentiates obese and lean humans and contributes to insulin resistance. Cell Metab. 2009; 9:311. [PubMed: 19356713]
26. Muegge BD, et al. Diet drives convergence in gut microbiome functions across mammalian phylogeny and within humans. Science. 2011; 332:970. [PubMed: 21596990]
27. Keenan MJ, et al. Effects of resistant starch, a non-digestible fermentable fiber, on reducing body fat. Obesity (Silver Spring). 2006; 14:1523. [PubMed: 17030963]
28. Zhou J, et al. Dietary resistant starch upregulates total GLP-1 and PYY in a sustained day-long manner through fermentation in rodents. Am J Physiol Endocrinol Metab. 2008; 295:E1160. [PubMed: 18796545]
29. Zhou J, et al. Failure to ferment dietary resistant starch in specific mouse models of obesity results in no body fat loss. J Agric Food Chem. 2009; 57:8844. [PubMed: 19739641]
30. Knights D, et al. Bayesian community-wide culture-independent microbial source tracking. Nat Methods. 2011; 8:761. [PubMed: 21765408]
31. Lessard JP, Fordyce JA, Gotelli NJ, Sanders NJ. Invasive ants alter the phylogenetic structure of ant communities. Ecology. 2009; 90:2664. [PubMed: 19886475]
32. Johnson MT, Stinchcombe JR. An emerging synthesis between community ecology and evolutionary biology. Trends Ecol Evol. 2007; 22:250. [PubMed: 17296244]
33. Webb CO, Pitman NC. Phylogenetic balance and ecological evenness. Syst Biol. 2002; 51:898. [PubMed: 12554456]
34. Turnbaugh PJ, et al. An obesity-associated gut microbiome with increased capacity for energy harvest. Nature. 2006; 444:1027. [PubMed: 17183312]
35. Gauffin Cano P, Santacruz A, Moya A, Sanz Y. Bacteroides uniformis CECT 7771 ameliorates metabolic and immunological dysfunction in mice with high-fat-diet induced obesity. PLoS One. 2012; 7:e41079. [PubMed: 22844426]
36. Duncan SH, et al. Contribution of acetate to butyrate formation by human faecal bacteria. Br J Nutr. 2004; 91:915. [PubMed: 15182395]
37. Mahowald MA, et al. Characterizing a model human gut microbiota composed of members of its two dominant bacterial phyla. Proc Natl Acad Sci U S A. 2009; 106:5859. [PubMed: 19321416]
38. Gao Z, et al. Butyrate improves insulin sensitivity and increases energy expenditure in mice. Diabetes. 2009; 58:1509. [PubMed: 19366864]
39. Lin HV, et al. Butyrate and propionate protect against diet-induced obesity and regulate gut hormones via free fatty acid receptor 3-independent mechanisms. PLoS One. 2012; 7:e35240. [PubMed: 22506074]

40. Kuribayashi H, Miyata M, Yamakawa H, Yoshinari K, Yamazoe Y. Enterobacteria-mediated deconjugation of taurocholic acid enhances ileal farnesoid X receptor signaling. Eur J Pharmacol. 2012; 697:132. [PubMed: 23051670]
41. Swann JR, et al. Systemic gut microbial modulation of bile acid metabolism in host tissue compartments. Proc Natl Acad Sci U S A. 2011; 108(Suppl 1):4523. [PubMed: 20837534]
42. Zhang Y, et al. Loss of FXR protects against diet-induced obesity and accelerates liver carcinogenesis in ob/ob mice. Mol Endocrinol. 2012; 26:272. [PubMed: 22261820]
43. Inagaki T, et al. Fibroblast growth factor 15 functions as an enterohepatic signal to regulate bile acid homeostasis. Cell Metab. 2005; 2:217. [PubMed: 16213224]
44. Li T, et al. Transgenic expression of cholesterol 7alpha-hydroxylase in the liver prevents high-fat diet-induced obesity and insulin resistance in mice. Hepatology. 2010; 52:678. [PubMed: 20623580]
45. Handelsman Y. Role of bile acid sequestrants in the treatment of type 2 diabetes. Diabetes Care. 2011; 34(Suppl 2):S244. [PubMed: 21525463]
46. Koves TR, et al. Peroxisome proliferator-activated receptor-gamma co-activator 1alpha-mediated metabolic remodeling of skeletal myocytes mimics exercise training and reverses lipid-induced mitochondrial inefficiency. J Biol Chem. 2005; 280:33588. [PubMed: 16079133]
47. Koves TR, et al. Mitochondrial overload and incomplete fatty acid oxidation contribute to skeletal muscle insulin resistance. Cell Metab. 2008; 7:45. [PubMed: 18177724]
48. Muoio DM, et al. Muscle-specific deletion of carnitine acetyltransferase compromises glucose tolerance and metabolic flexibility. Cell Metab. 2012; 15:764. [PubMed: 22560225]
49. Bakken JS, et al. Treating Clostridium difficile infection with fecal microbiota transplantation. Clin Gastroenterol Hepatol. 2011; 9:1044. [PubMed: 21871249]
50. Turnbaugh PJ, et al. The effect of diet on the human gut microbiome: a metagenomic analysis in humanized gnotobiotic mice. Sci Transl Med. 2009; 1:6ra14.
51. Ahern PP, et al. Interleukin-23 drives intestinal inflammation through direct activity on T cells. Immunity. 2010; 33:279. [PubMed: 20732640]
52. Esplugues E, et al. Control of TH17 cells occurs in the small intestine. Nature. 2011; 475:514. [PubMed: 21765430]
53. Edgar RC. Search and clustering orders of magnitude faster than BLAST. Bioinformatics. 2010; 26:2460. [PubMed: 20709691]
54. Caporaso JG, et al. PyNAST: a flexible tool for aligning sequences to a template alignment. Bioinformatics. 2010; 26:266. [PubMed: 19914921]
55. DeSantis TZ, et al. Greengenes, a chimera-checked 16S rRNA gene database and workbench compatible with ARB. Appl Environ Microbiol. 2006; 72:5069. [PubMed: 16820507]
56. Cole JR, et al. The ribosomal database project (RDP-II): introducing myRDP space and quality controlled public data. Nucleic Acids Res. 2007; 35:D169. [PubMed: 17090583]
57. Caporaso JG, et al. QIIME allows analysis of high-throughput community sequencing data. Nat Methods. 2010; 7:335. [PubMed: 20383131]
58. Kuczynski J, et al. Direct sequencing of the human microbiome readily reveals community differences. Genome Biol. 2010; 11:210. [PubMed: 20441597]
59. Oksanen, JGBF.; Kndt, R.; Legendre, P.; Minchin, PR.; O'Hara, RB.; Simpson, GL.; Solymos, P.; Stevens, MHH.; Wagner, H. 2011. http://CRAN.R-project.org/package=veganvol. R package version 2.0-2
60. Faith JJ, McNulty NP, Rey FE, Gordon JI. Predicting a human gut microbiota's response to diet in gnotobiotic mice. Science. 2011; 333:101. [PubMed: 21596954]
61. McNulty NP, et al. The impact of a consortium of fermented milk strains on the gut microbiome of gnotobiotic mice and monozygotic twins. Sci Transl Med. 2011; 3:106ra106.
62. Rey FE, et al. Dissecting the in vivo metabolic potential of two human gut acetogens. J Biol Chem. 2010; 285:22082. [PubMed: 20444704]
63. Langmead B, Salzberg SL. Fast gapped-read alignment with Bowtie 2. Nat Methods. 2012; 9:357. [PubMed: 22388286]

64. Benhamed F, et al. The lipogenic transcription factor ChREBP dissociates hepatic steatosis from insulin resistance in mice and humans. J Clin Invest. 2012; 122:2176. [PubMed: 22546860]

65. Goodman AL, et al. Extensive personal human gut microbiota culture collections characterized and manipulated in gnotobiotic mice. Proc Natl Acad Sci U S A. 2011; 108:6252. [PubMed: 21436049]

66. Delcher AL, Bratke KA, Powers EC, Salzberg SL. Identifying bacterial genes and endosymbiont DNA with Glimmer. Bioinformatics. 2007; 23:673. [PubMed: 17237039]

67. Lowe TM, Eddy SR. tRNAscan-SE: a program for improved detection of transfer RNA genes in genomic sequence. Nucleic Acids Res. 1997; 25:955. [PubMed: 9023104]

68. Lagesen K, et al. RNAmmer: consistent and rapid annotation of ribosomal RNA genes. Nucleic Acids Res. 2007; 35:3100. [PubMed: 17452365]

69. Cantarel BL, et al. The Carbohydrate-Active EnZymes database (CAZy): an expert resource for Glycogenomics. Nucleic Acids Res. 2009; 37:D233. [PubMed: 18838391]

70. Bostrom P, et al. A PGC1-alpha-dependent myokine that drives brown-fat-like development of white fat and thermogenesis. Nature. 2012; 481:463. [PubMed: 22237023]

71. Seale P, et al. PRDM16 controls a brown fat/skeletal muscle switch. Nature. 2008; 454:961. [PubMed: 18719582]

72. Lozupone C, Knight R. UniFrac: a new phylogenetic method for comparing microbial communities. Appl Environ Microbiol. 2005; 71:8228. [PubMed: 16332807]

73. Lozupone CA, et al. The convergence of carbohydrate active gene repertoires in human gut microbes. Proc Natl Acad Sci U S A. 2008; 105:15076. [PubMed: 18806222]

74. Knights D, Costello EK, Knight R. Supervised classification of human microbiota. FEMS Microbiol Rev. 2011; 35:343. [PubMed: 21039646]

75. Horner-Devine MC, Bohannan BJ. Phylogenetic clustering and overdispersion in bacterial communities. Ecology. 2006; 87:S100. [PubMed: 16922306]

76. Furet JP, et al. Differential adaptation of human gut microbiota to bariatric surgery-induced weight loss: links with metabolic and low-grade inflammation markers. Diabetes. 2010; 59:3049. [PubMed: 20876719]

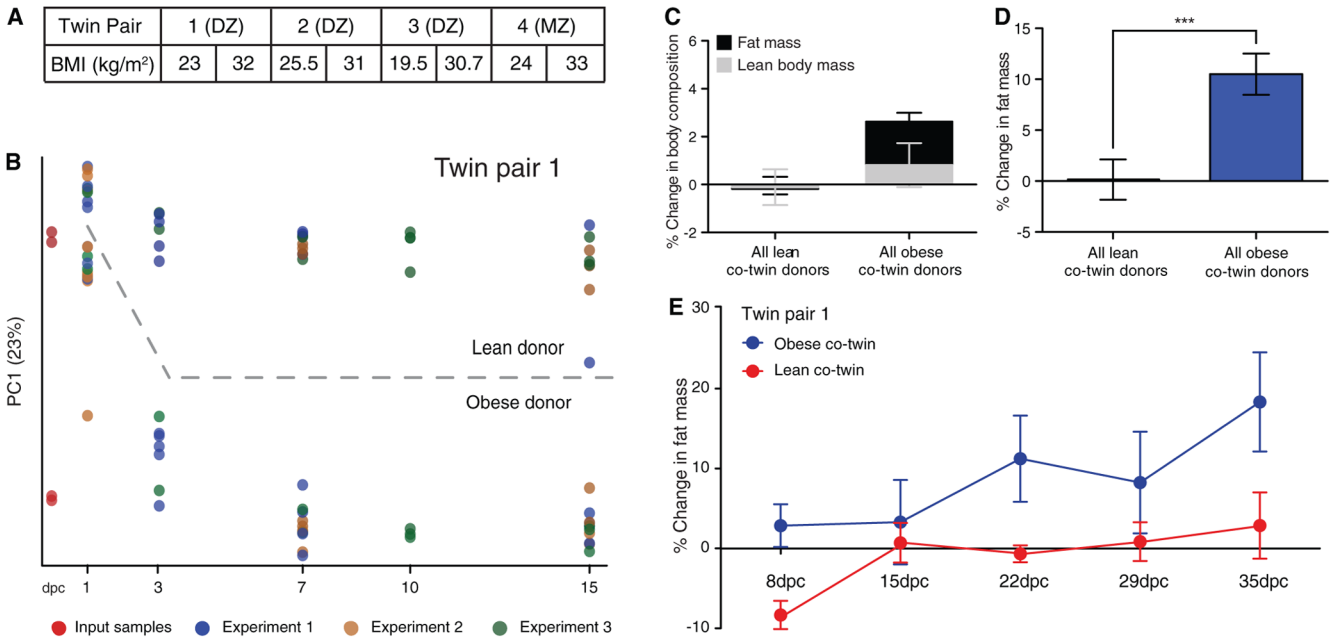

Fig. 1. Reliable replication of human donor microbiota in gnotobiotic mice

(**A**) Features of the four discordant twin pairs. (**B**) Assembly of bacterial communities in mice that had received intact uncultured fecal microbiota transplants from the obese and lean co-twins in DZ pair 1. PCoA plot based on an unweighted UniFrac distance matrix and 97%ID OTUs present in sampled fecal communities. Circles correspond to a single fecal sample obtained at a given time point from a given mouse and are colored according to the experiment (n=3 independent experiments). Note that assembly is reproducible within members of a group of mice that have received a given microbiota, and between experiments. (**C**) Body composition, defined by qMR, was performed one day and 15 days post colonization (dpc) of each mouse in each recipient group. Mean values (± SEM) are plotted for the percent increase in fat mass and lean body mass at 15 dpc for all recipient mice of each of the four obese co-twins' or lean co-twins' fecal microbiota, normalized to the initial body mass of each recipient mouse. A two-way ANOVA indicated that there was a significant donor effect ($p \leq 0.05$), driven by a significant difference in adiposity between mice colonized with a lean or obese co-twin donor's fecal microbiota (adjusted $p \leq 0.05$; Šidák's multiple comparisons test). **(D)** Mean values (± SEM) are plotted for the percent change in fat mass at 15 dpc for all recipient mice of each of the four obese co-twins' or lean co-twins' fecal microbiota. Data are normalized to initial fat mass (n=3–12 animals/donor microbiota; 51–52 mice/BMI bin; total of 103 mice). ***, $p \leq 0.001$, as judged by a one-tailed unpaired Student's *t*-test. (**E**) Prolonged time course study for recipients of fecal microbiota from co-twins in discordant DZ pair 1 (mean values ± SEM plotted; n=4 mice/donor microbiota). The difference between the gain in adiposity calculated relative to initial fat mass (1 dpc) between the two recipient groups of mice is statistically significant ($p \leq 0.001$, two-way ANOVA).

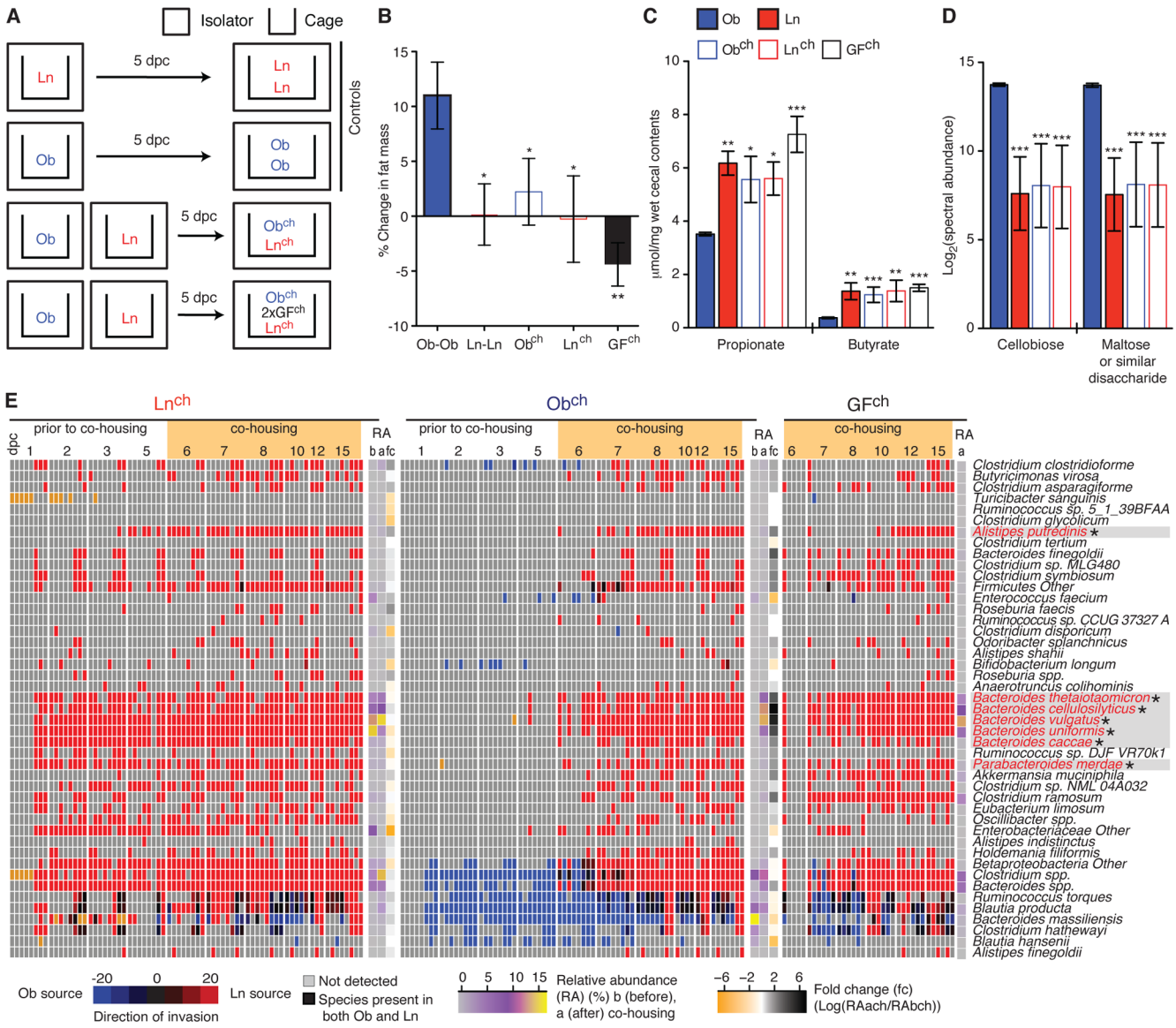

Fig. 2. Co-housing Ob^{ch} and Ln^{ch} mice transforms the adiposity phenotype of cagemates harboring the obese co-twin's culture collection to a lean-like state

(A) Design of co-housing experiment. 8-week-old, male, germ-free C57BL/6J mice received culture collections from the lean (Ln) twin or the obese (Ob) co-twin in DZ twin pair 1. Five days after colonization, mice were co-housed in one of three configurations: control groups consisted of dually-housed Ob-Ob or Ln-Ln cagemates; the experimental group consisted of dually-housed Ob^{ch}-Ln^{ch} cagemates (data shown from 5 cages/experiment; 2 independent experiments) or Ob^{ch}-Ln^{ch}- GF^{ch}-GF^{ch} cagemates (n=3 cages/experiment). All mice were fed a LF/HPP diet. (**B**) Effects of co-housing on fat mass. Changes from the first day after co-housing to 10 d after co-housing were defined using whole body qMR. *, $p \leq 0.05$, **, $p \leq 0.01$ compared to Ob-Ob controls, as defined by one-tailed unpaired Student's *t*-test. **(C)** Targeted GC/MS analysis of cecal short chain fatty acids. Compared to Ob-Ob controls, the concentrations of propionate and butyrate were significantly higher in the ceca of Ob^{ch}, Ln-Ln, Ln^{ch}, and GF^{ch} mice. (**D**) Nontargeted GC/MS analysis of cecal levels of cellobiose and 'maltose or a similar disaccharide'. *, $p \leq 0.05$; **, $p \leq 0.01$. (**E**) Evidence that bacterial

species from the Ln^{ch} microbiota invade the Ob^{ch} microbiota. Shown are SourceTracker-based estimates of the proportion of bacterial taxa in a given community that are derived from a cagemate. For Ob^{ch}-Ln^{ch} co-housing experiments, Ob^{ch} or Ln^{ch} microbiota were designated as sink communities, while the gut microbiota Ob-Ob or Ln-Ln controls [at 5 days post colonization (dpc)] were considered source communities. Red indicates species derived from the Ln^{ch} gut microbial community. Blue denotes species derived from the Ob^{ch} microbiota. Black denotes unspecified source (i.e. both communities have this species), while orange indicates an uncertain classification by the SourceTracker algorithm. An asterisk placed next to a species indicates that it is a successful invader as defined in the text. Average relative abundance (RA) in the fecal microbiota is shown **b**efore co-housing (**b,** at 5 dpc) and **a**fter co-housing (**a**, at 15 dpc). The average fold-change (fc) in relative abundance for a given taxon, for all time points before and after co-housing is shown (excluding the first two days immediately after gavage of the microbiota and immediately after initiation of co-housing).

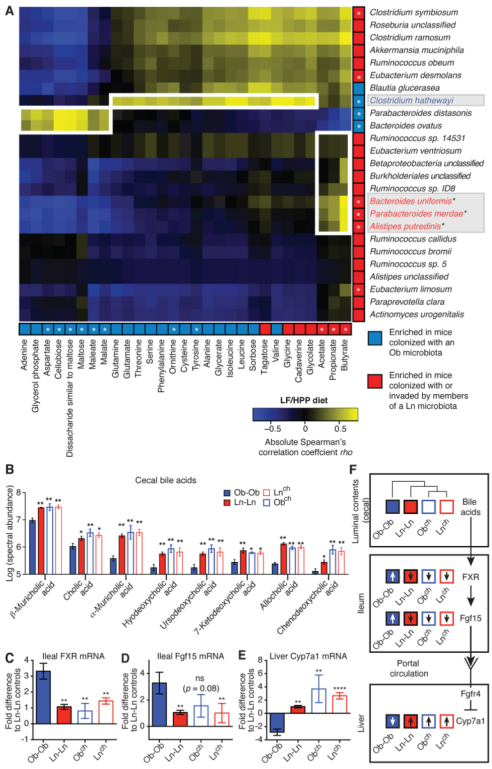

Fig. 3. Effect of co-housing on metabolic profiles in mice consuming a LF/HPP diet

(**A**) Spearman's correlation analysis of cecal metabolites and cecal bacterial species-level taxa in samples collected from Ob^{ch}, Ln^{ch}, GF^{ch}, $Ln39^{ch}$, Ob^{chLn39} cagemates and from Ob-Ob and Ln-Ln controls (correlations with $p \leq 0.0001$ are shown). Taxonomic assignments were made using a modified NCBI taxonomy (23). Bacterial species and cecal metabolites enriched in animals colonized with either the Ln or Ob culture collections are colored red and blue, respectively. An asterisk in the colored box indicates that that a taxon or metabolite is significantly enriched in mice colonized with Ln (red) or Ob (blue) culture collections. Bacterial species colored red denote significant invaders from Ln^{ch} mouse into the gut microbiota of Ob^{ch} cagemates. (**B**) Cecal bile acids measured by UPLC-MS. Note that levels are plotted as log transformed spectral abundances. Significance of differences relative to Ob-Ob controls were defined using a two-way ANOVA with Holm- Šidák's correction for multiple hypotheses; *, $p \leq 0.05$; **, $p \leq 0.01$; ****, $p \leq 0.001$. (**C, D**) Quantitative RT-PCR assays of FXR and Fgf15 mRNA levels in the distal ileum. Data are normalized to Ln-Ln controls. (**E**) qRT-PCR of hepatic Cyp7a1 mRNA, normalized to Ln-Ln controls. *, $p \leq 0.05$; **, $p \leq 0.01$; ****, $p \leq 0.001$ (defined by one-tailed, unpaired Student's *t*-test using Ob-Ob mice as reference controls). (**F**) Correlating cecal bile acid profiles with the FXR-Fgf15-Cyp7A signaling pathway in the different groups of mice. The dendrogram in the upper panel highlights the differences in the profiles of 37 bile acid species between Ob-Ob controls versus the other three treatment groups. The dendrogram was calculated using the Bray-Curtis dissimilarity index and the average relative abundance of each bile acid species among all mice belonging to a given treatment group.

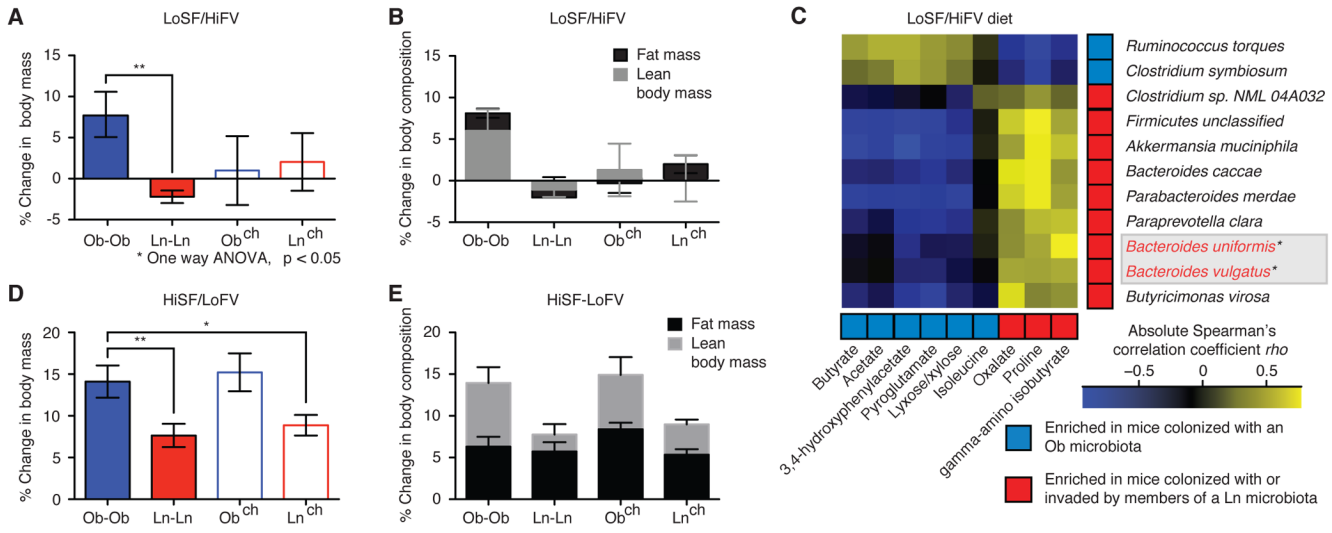

Fig. 4. Effects of NHANES-based LoSF/HiFV and HiSF/LoFV diets on bacterial invasion, body mass and metabolic phenotypes

(**A, B**) Mean ± SEM percent change in total body mass (panel A) and body composition (fat and lean body mass, normalized to initial body mass on day 4 after gavage, panel B) occurring between 4d and 14d after colonization with culture collections from the Ln or Ob co-twin in DZ pair 1. Co-housing Ln and Ob mice prevents an increased body mass phenotype in Ob^{ch} cagemates fed the representative human diet that was low in saturated fats and high in fruits and vegetables (LoSF/HiFV) (n=3–5 cages/treatment group; 26 animals in total). **, $p \leq 0.01$ based on a one way ANOVA after Fisher's LSD test (also see table S13). (**C**) Spearman's correlation analysis between bacterial species-level taxa and metabolites in cecal samples collected from mice, colonized with culture collections from DZ twin pair 1 Ln and Ob co-twins and fed a LoSF/HiFV diet. Red and blue squares indicate metabolites or taxa that are significantly enriched in samples collected from dually-housed Ln-Ln or Ob-Ob controls respectively. (**D, E**) Mean± SEM of changes in body mass and body composition in mice colonized with intact uncultured microbiota from DZ twin pair 2 and fed the representative human diet that was high in saturated fats and low in fruits and vegetables (HiSF/LoFV). Ob-Ob controls have greater lean body mass than Ln-Ln controls but this phenotype is not rescued in Ob^{ch} animals (see table S14 for statistics). Note that the HiSF/LoFV diet produces a significantly greater increase in body mass, specifically fat mass, in mice harboring the lean co-twins microbiota (Ln-Ln and Ln^{ch}) compared to when they are fed the LoSF/HiFV diet (see panels A, B versus D, E; two-way ANOVA with Holm-Sidak's correction for multiple hypotheses).

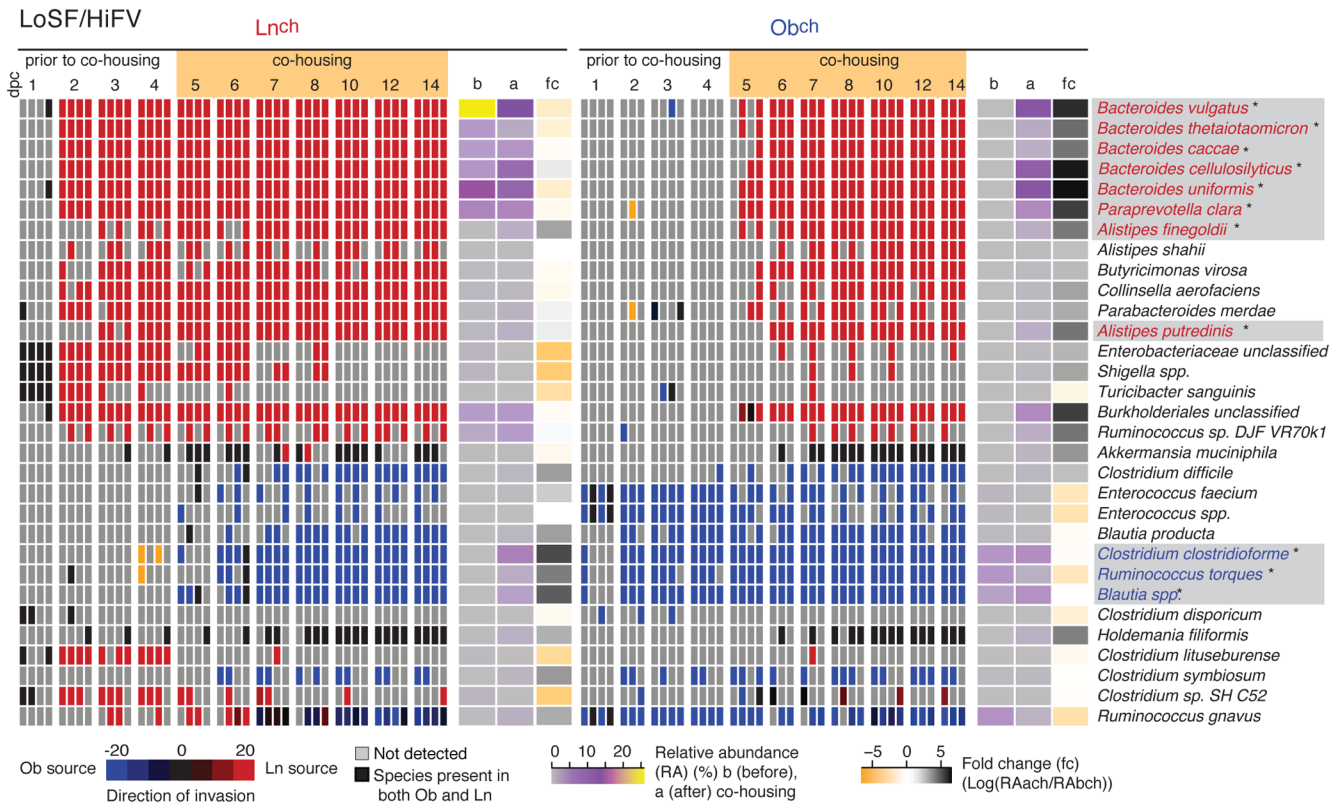

Fig. 5. Invasion analysis of species-level taxa in Ob^{ch} or Ln^{ch} mice fed the NHANES-based LoSF/HiFV diet

Red indicates species derived from the Ln^{ch} gut microbial community. Blue denotes species derived from the Ob^{ch} microbiota. The mean relative abundance of each species-level taxon **b**efore (**b**; 3 and 4 dpc) and **a**fter (**a**; 8, 10 and 14 dpc) co-housing is noted. Fold-change (**fc**) in relative abundance of taxa before and after colonization (see legend to Fig. 2E). An asterisk (*) denotes bacterial species that satisfy our criteria for classification as successful invaders (see text).

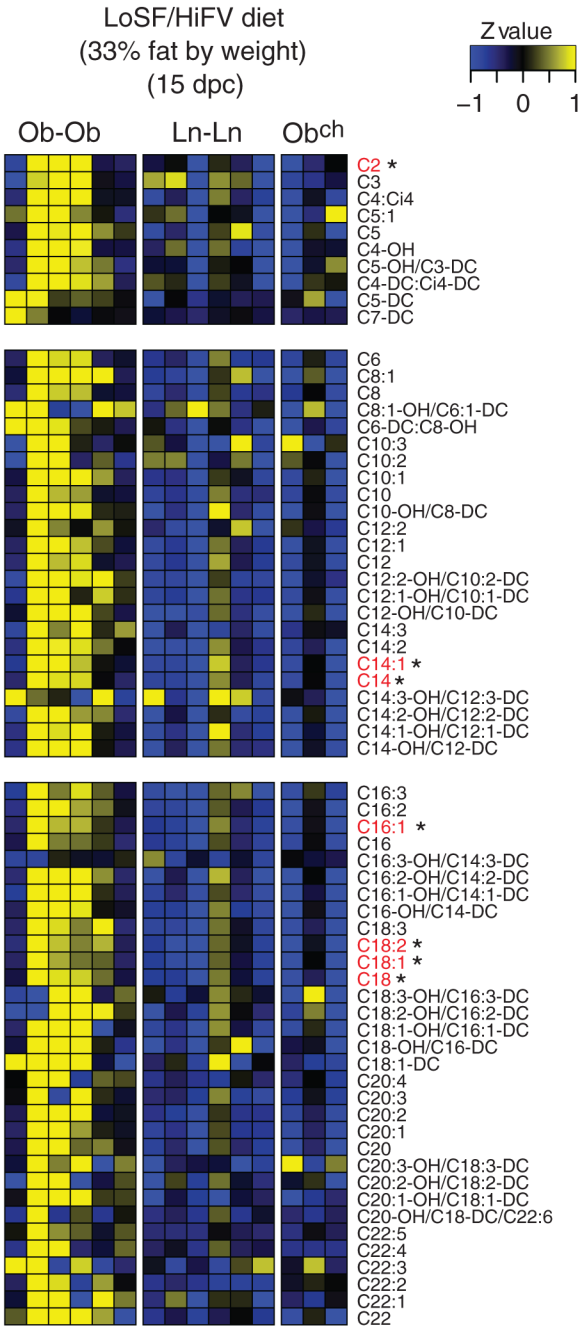

Fig. 6. Acylcarnitine profile in the skeletal muscle of mice colonized with the Ob or Ln culture collections from DZ twin pair 1 and fed the LoSF/HiFV diet

Each column represents a different animal and each row a different acylcarnitine. The identities and levels of these acylcarnitines were determined by targeted MS/MS (see table S15 for mean values ± SEM for each treatment group). A two-way ANOVA with Holm-Šidák's correction was used to calculate whether the level of each acylcarnitine was significantly different between Ob-Ob versus Ln-Ln, Ln^{ch} or Ob^{ch} animals. * $p \leq 0.05$.